Available at
www.ComputerScienceWeb.com
POWERED BY SCIENCE @ DIRECT®

ELSEVIER

Pattern Recognition Letters 24 (2003) 1513–1521

Pattern Recognition Letters

www.elsevier.com/locate/patrec

Texture classification using wavelet transform

S. Arivazhagan [a,*], L. Ganesan [b]

[a] Department of Electronics and Communication Engineering, Mepco Schlenk Engineering College, Amathur (P.O.), Sivakasi 626 005, India

[b] Department of Computer Science and Engineering, Government College of Engineering, Tirunelveli 627 007, India

Received 1 February 2002; received in revised form 7 November 2002

Abstract

Today, texture analysis plays an important role in many tasks, ranging from remote sensing to medical imaging and query by content in large image data bases. The main difficulty of texture analysis in the past was the lack of adequate tools to characterize different scales of textures effectively. The development in multi-resolution analysis such as Gabor and wavelet transform help to overcome this difficulty. This paper describes the texture classification using (i) wavelet statistical features, (ii) wavelet co-occurrence features and (iii) a combination of wavelet statistical features and co-occurrence features of one level wavelet transformed images with different feature databases. It is found that, the results of later method are promising.

Keywords: Texture; Wavelet; Wavelet statistical feature; Wavelet co-occurrence feature; Feature extraction; Texture classification

1. Introduction

For years, researchers have attempted to duplicate the ability of the human brain, to understand the content of images by interpreting the shape and texture of the object in the scene, by developing image understanding algorithms for applications including robotic vision, industrial monitoring, remote sensing, assisted medical diagnosis and automated target recognition (e.g., Kaplan, 1999, p. 1572). In spite of the importance of textures in many real and synthetic images, it is very difficult to give a universal definition of texture due to the diversity of patterns in several natural and artificial textures. According to Sklansky (1978), "An image region has a constant texture if a set of local properties in that region is constant, slowly varying or approximately periodic". The local statistics or property that is repeated over the textured region is called a texture element or texel. It must be noted that the texture has both local and global meaning i.e., it is characterized by invariance of certain local attributes that are distributed over a region of an image (e.g., Raghu and Yegnanarayana, 1996, p. 1625).

Analysis of texture requires the identification of proper attributes or features that differentiate the textures for classification, segmentation and

* Corresponding author.
E-mail address: s_arivu@yahoo.com (S. Arivazhagan).

0167-8655/03/$ - see front matter © 2002 Elsevier Science B.V. All rights reserved.
PII: S0167-8655(02)00390-2

recognition. The features are assumed to be uniform within the regions containing the same texture. Various feature extraction and classification techniques have been suggested in the past for the purpose of texture analysis. Initially, texture analysis was based on the first order or second order statistics of textures (e.g. Haralick et al., 1973; Weszka et al., 1976; Davis et al., 1979; Faugeras and Pratt, 1980; Chen and Pavlidis, 1983). It is well known that the co-occurrence matrix features are first proposed by Haralick et al. (1973). However, there are 14 features are to be computed that too for different distances at different orientations which increases the computational and time complexity. Even if all the features are used, the correct classification rate of 60–70% was only reported in the literature. Then, Gaussian Markov random fields (GMRF) and Gibbs random fields were proposed to characterize textures (e.g. Cross and Jain, 1983; Kashyap and Khotanzed, 1986; Chellappa and Chatterjee, 1986; Derin and Elliot, 1987; Cohen et al., 1991; Manjunath and Chellappa, 1991). Later, local linear transformations are used to compute texture features (e.g. Laws, 1980; Unser, 1986). The above traditional statistical approaches to texture analysis such as co-occurrence matrices, second order statistics, GMRF and local linear transforms are restricted to the analysis of spatial interactions over relatively small neighborhoods on a single scale. As a consequence, their performance is best for the analysis of micro-textures only (e.g., Unser, 1995, p. 1549).

More recently methods based on multi-resolution or multi-channel analysis such as Gabor filters and wavelet transform have received a lot of attention (e.g. Unser and Eden, 1989; Bovik et al., 1990; Chang and Jay Kuo, 1993; Unser, 1995; Teuner et al., 1995; Haley and Manjunath, 1995; Manjunath and Ma, 1996; Wu and Wei, 1996; Raghu and Yegnanarayana, 1996; Van de Wouwer et al., 1999). A major disadvantage in using Gabor transform is that the output of Gabor filter banks are not mutually orthogonal, which may result in a significant correlation between texture features. Moreover, these transformations are usually not reversible, which limits their applicability for texture synthesis. Most of these can be avoided if one uses the wavelet transform, which provides a precise and unifying frame work for the analysis and characterization of a signal at different scales (Unser, 1995, p. 16–19). Another advantage of wavelet transform over Gabor filter is the low pass and high pass filters used in the wavelet transform remain the same between two consecutive scales while the Gabor approach requires filters of different parameters (e.g. Chang and Jay Kuo, 1993). In other words, Gabor filters require proper tuning of filter parameters at different scales.

According to Chang and Jay Kuo (1993), the texture classification rate of the conventional pyramid structured wavelet transform is higher than that of other methods such as Gabor filter and Tree structured wavelet transform, when more number of features are used. Later, texture classification is done using wavelet frames (e.g. Unser, 1995). Then, Van de Wouwer et al. (1999) used histogram and co-occurrence signatures for texture characterization and Wang and Liu (1999) proposed the concept of multi-resolution Markov random field (MRMRF) modeling in which the sub-bands of wavelet decomposed textures are modeled with MRF and the corresponding Gibbs cliques potential parameters are used as features for classification.

The objective of this research is twofold. Firstly, the discrete wavelet transform (DWT) features are shown to be used for texture characterization and classification. Secondly, the usage of the co-occurrence features, computed out of the sub-bands of wavelet transformed images, for texture classification is explained. The intuition behind this is the chances of correct classification will be considerably improved if higher order statistical features are used, as they will normally have good discriminating ability than the lower order one.

In this paper, the DWT is applied on a set of texture images and statistical features such as mean and standard deviation are extracted from the approximation and detail regions of DWT decomposed images, at different scales. The various combinations of the above statistical features are applied for texture classification and a set of best feature vectors are chosen. In order to improve the success rate of classification, the co-occurrence matrix is calculated for original image, approximation and detail sub-bands of 1-level DWT decomposed images and additional features are extracted. These additional features are combined with the above chosen best wavelet statistical feature (WSF) sets and a detailed analysis is done using three different feature databases. It is found that the success rate is improved much by combining wavelet statistical and co-occurrence matrix features.

This paper is organized as follows: In Section 2, the theory of DWT is briefly reviewed. The feature extraction and texture classification are explained in Section 3. In Section 4, texture classification experimental results using various feature sets are discussed in detail. Finally, concluding remarks are given in Section 5.

2. Discrete wavelet transform

The image is actually decomposed i.e., divided into four sub-bands and critically sub-sampled by applying DWT as shown in Fig. 1(a). These sub-bands labeled LH1, HL1 and HH1 represent the finest scale wavelet coefficients i.e., detail images while the sub-band LL1 corresponds to coarse level coefficients i.e., approximation image. To obtain the next coarse level of wavelet coefficients, the sub-band LL1 alone is further decomposed and critically sampled. This results in a two-level wavelet decomposition as shown in Fig. 1(b). Similarly, to obtain further decomposition, LL2 will be used. This process continues until some final scale is reached. The values or transformed coefficients in approximation and detail images (sub-band images) are the essential features, which are shown here as useful for texture analysis and discrimination. As micro-textures or macro-textures have non-uniform gray level variations, they are statistically characterized by the features in approximation and detail images. In other words, the values in the sub-band images or their combinations or the derived features from these bands uniquely characterize a texture. The features obtained from these wavelet transformed images are shown to be used for texture analysis, namely, classification and are discussed in the next section.

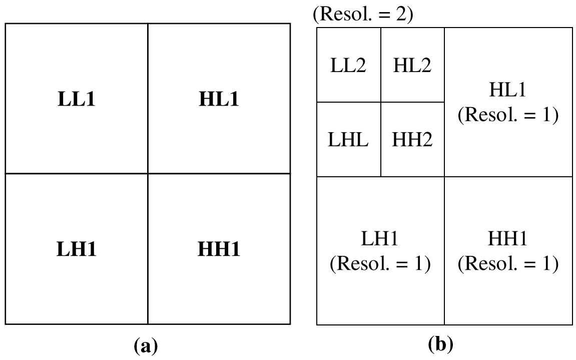

Fig. 1. Image decomposition. (a) One-level, (b) two level.

3. Feature extraction and texture classification

The steps involved in texture training and texture classification are shown in Fig. 2(a) and (b) respectively.

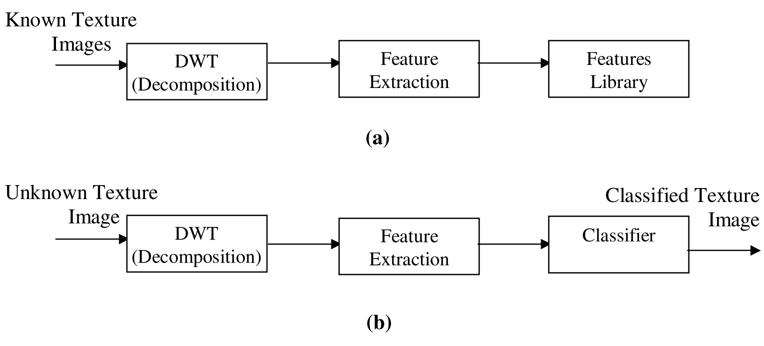

Fig. 2. (a) Texture training steps, (b) texture classification steps.

Texture training: In the texture training, the known texture images are decomposed using DWT. Then, mean and standard deviation of approximation and detail sub-bands of three level decomposed images (i.e., LLk, LHk, HLk and HHk; for $k = 1, 2, 3$) are calculated as features using the formulas given in the Eqs. (1) and (2) respectively and stored in features library.

$$\text{mean } (m) = \frac{1}{N^2} \sum_{i,j=1}^{N} p(i,j) \tag{1}$$

Standard deviation (sd)

$$= \sqrt{\frac{1}{N^2} \sum_{i,j=1}^{N} [p(i,j) - m]^2} \tag{2}$$

where $p(i,j)$ is the transformed value in (i,j) for any sub-band of size $N \times N$. Using this procedure, from any texture image, the features (upto k-level sub-bands) are computed and stored in the features library which are further used in texture classification phase. Using a combination of the above WSFs, texture classification is performed which yielded good result.

In order to improve the correct classification rate further, it is proposed to find co-occurrence matrix features for original image, approximation and detail sub-bands of 1-level DWT decomposed images (i.e., LL1, LH1, HL1 and HH1). The various co-occurrence features such as contrast, energy, entropy, local homogeneity, cluster shade, cluster prominence and maximum probability, as suggested by Haralick et al. (1973), are calculated from the co-occurrence matrix $C(i,j)$ using the formulas given in Appendix A.

Texture classification: Here, the unknown texture is decomposed using DWT and a similar set of wavelet statistical and co-occurrence matrix features are extracted and compared with the corresponding feature values stored in the features library using a distance vector formula, given in Eq. (3).

$$D(i) = \sum_{j=1}^{\text{No. of features}} abs\left[f_j(x) - f_j(i)\right] \tag{3}$$

where $f_j(x)$ represents the features of unknown texture while $f_j(i)$ represents the features of known ith texture in the library. Then, the unknown texture is classified as ith texture, if the distance $D(i)$ is minimum among all textures, available in the library.

4. Experimental results and discussion

Experiments are conducted with 20 monochrome texture images, each of size 512×512, obtained from VisTex (1995) Color image database shown in Fig. 3. For comparative analysis, texture classification is done using different feature vectors for three different feature databases.

The first feature database (Feat-DB1) is created from 20 512×512 original texture images by extracting (i) 24 WSFs such as mean and standard deviation of LLk, LHk, HLk and HHk (for $k = 1, 2, 3$) sub-bands of three-level DWT (Symlet—tab 20 filter) decomposed texture images and (ii) 35 wavelet co-occurrence features (WCF) such as contrast, energy, entropy, local homogeneity, cluster shade, cluster prominence and maximum probability, derived from co-occurrence matrices, computed for different angles (i.e., $\theta = 0°$, 45°, 90° and 135°) and averaged, of original images, approximation and detail sub-bands of 1-level DWT decomposed texture images.

The second feature database (Feat-DB2) is created from a total of 1680 image regions of 20 texture images, constructed by dividing each 512×512 texture image into non-overlapping 4 256×256, 16 128×128 and 64 64×64 image regions and by extracting 24 WSFs and 35 WCFs, averaged over these 84 image regions.

The third feature database (Feat-DB3) is obtained again from a total of 1680 image regions and it consists of three sub-databases derived by extracting 24 WSFs and 35 WCFs, averaged over 4 (256×256), 16 (128×128) and 64 (64×64) image regions respectively and either all these three different sub-databases are used based on the size of unknown image (or) one at a time during the classification.

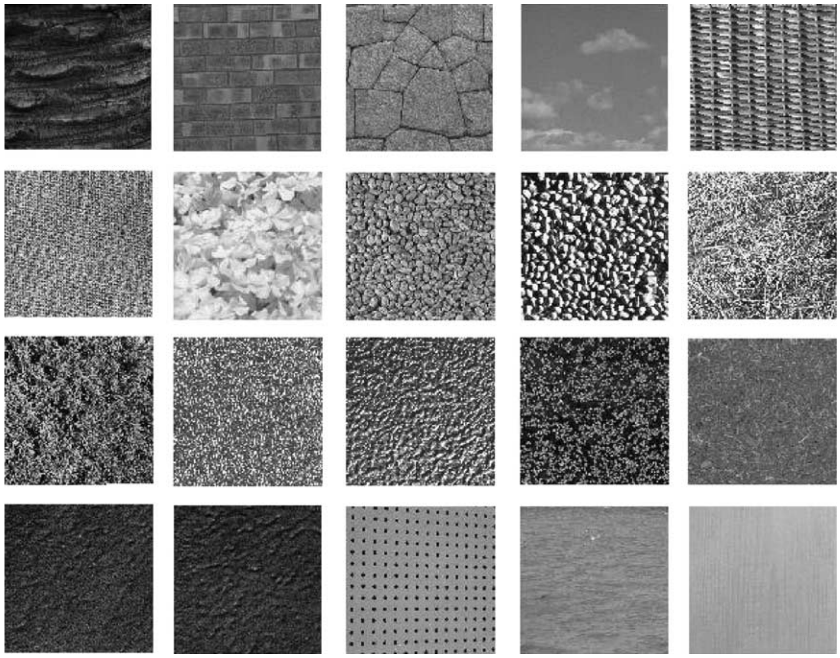

Fig. 3. Texture images. From left–right and top–bottom: Bark.0006, Brick.0000, Brick.0004, Clouds.0001, Fabric.0013, Fabric.0017, Flowers.0006, Food.0000, Food.0001, Grass.0001, Leaves.0012, Metal.0002, Metal.0004, Misc.0001, Misc.0002, Sand.0000, Sand.0002, Tile.0008, Water.0005, Wood.0002.

Texture classification is done with a total of 1680 (i.e., 20×84) image regions of 20 texture images, shown in Fig. 3, In the first instance, texture classification is done with Feat-DB1 using 14 WSFs (feature vector—F1), 17 WCFs (feature vector—F2) and a combination of WSFs and WCFs (feature vector—F3) and the results are summarized in Table 1, where each entry corresponds to the average correct classification rate of all the 84 image regions of different sizes, discussed earlier. From the Table 1, it is observed that the mean success rate for feature vectors F1, F2 and F3 are 92.02%, 87.86% and 97.68% respectively.

In the second instance, again the combination of WSFs and WCFs (feature vector—F4) are used to classify images with Feat-DB2 and it is found that the mean success rate is 97.26%. Next, classification is carried out with Feat-DB3 using the same combination of WSFs and WCFs. In feature vector F5, the 1680 image regions are classified by comparing one of the three feature sub-databases based on their size. But, in feature vectors F6, F7 and F8 all the 1680 image regions are classified by comparing trained averaged features of 64×64, 128×128 and 256×256 image regions respectively, irrespective of their size. The mean success rate of feature vectors F5, F6, F7 and F8 are 97.14%, 96.96%, 97.56% and 97.80% respectively. The graphical analysis of texture classification results are shown is Fig. 4.

From the Table 1 and from Fig. 4, it is found that when classification is carried out with Feat-DB1 (i.e., features derived from 20 original images), the mean success rate is higher i.e., 97.68% for combination of wavelet statistical and co-occurrence features (feature vector F3). But, when classification is done with Feat-DB2 (i.e., averaged features derived from 1680 image regions) the mean success rate is slightly reduced to 97.26%. However, for classification using Feat-DB3, it is observed that (i) the mean success rate is highest i.e., 97.80% for feature vector F8, when

Table 1
Results of texture classification using wavelet statistical and co-occurrence features (with 1680 image regions)

Sl. no.	Images	Correct classification (%)							
		Feature vectors							
		F1	F2	F3	F4	F5	F6	F7	F8
1	Bark.0006	46.43	90.48	90.48	91.67	92.86	92.86	91.67	91.67
2	Brick.0000	97.62	96.43	100	100	100	100	100	100
3	Brick.0004	82.14	98.81	100	100	100	100	100	100
4	Clouds.0001	79.76	90.48	96.43	96.43	96.43	94.05	96.43	97.62
5	Fabric.0013	97.62	96.43	100	97.62	97.62	97.62	100	100
6	Fabric.0017	100	96.43	97.62	97.62	97.62	97.62	97.62	97.62
7	Flowers.0006	94.05	35.71	98.81	98.81	98.81	98.81	98.81	98.81
8	Food.0000	100	92.86	98.81	98.81	98.81	98.81	98.81	98.81
9	Food.0001	100	73.81	96.43	96.43	97.62	97.62	97.62	97.62
10	Grass.0001	86.9	77.38	80.95	78.57	78.57	78.57	79.76	80.95
11	Leaves.0012	90.48	91.67	96.43	94.05	91.67	91.67	94.05	96.43
12	Metal.0002	100	100	100	100	100	100	100	100
13	Metal.0004	86.9	100	100	98.81	98.81	98.81	100	100
14	Misc.0001	100	84.52	100	100	100	100	100	100
15	Misc.0002	97.62	91.67	98.81	98.81	97.62	97.62	98.81	98.81
16	Sand.0000	96.43	95.24	100	100	100	100	100	100
17	Sand.0002	89.29	91.67	98.81	98.81	97.62	96.43	97.62	97.62
18	Tile.0008	97.62	97.62	100	100	100	100	100	100
19	Water.0005	97.62	83.33	100	98.81	98.81	98.81	100	100
20	Wood.0002	100	72.62	100	100	100	100	100	100
Number of image regions correctly classified		1546	1476	1641	1634	1632	1628	1639	1643
Mean success rate		92.02	87.86	97.68	97.26	97.14	96.96	97.56	97.80

F1 = wavelet statistical features (WSF)—(trained by features of 512×512 original images: Feat-DB1).
F2 = wavelet co-occurrence features (WCF)—(trained by features of 512×512 original images: Feat-DB1).
F3 = WSFs + WCFs (trained by features of 512×512 original images: Feat-DB1).
F4 = WSFs + WCFs (trained by averaged features of 4 256×256, 16 128×128 and 64 64×64 non-overlapping image regions: Feat-DB2).
F5 = WSFs + WCFs (trained by three averaged feature sub-databases of 4 256×256, 16 128×128 and 64 64×64 non-overlapped image regions: Feat-DB3).
F6 = WSFs + WCFs (trained by averaged features of 64 64×64 non-overlapping image regions: Feat-DB3).
F7 = WSFs + WCFs (trained by averaged features of 16 128×128 non-overlapping image regions: Feat-DB3).
F8 = WSFs + WCFs (trained by averaged features of 4 256×256 non-overlapping image regions: Feat-DB3).

classification is done by comparing 1680 image regions with averaged features of 256×256 image regions; (ii) the mean success rates are 96.96% and 97.56% for feature vectors F6, F7, when classification is carried out with averaged features of 64×64 and 128×128 size image regions respectively and (iii) for feature vector F5, the mean classification rate is 97.14% when classification is carried out with averaged features of either 64×64 or 128×128 or 256×256 image regions based on the size of unknown image.

5. Conclusion

From the exhaustive experiments conducted with texture images, it is concluded that:

(i) When classification is done with feature database 1, the mean success rate is improved to 97.68% for a combination of WSFs and WCFs compared to that of WSFs (or) WCFs.
(ii) When feature database 2 is used for classification, the mean success rate is slightly reduced to 97.26%.

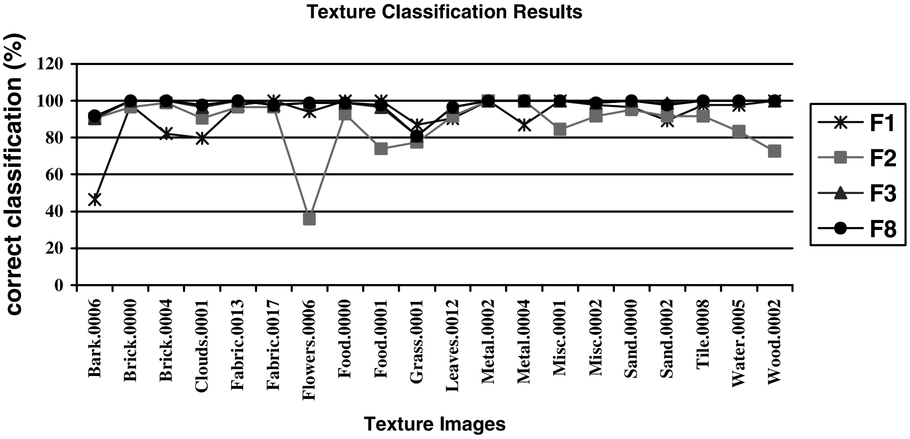

(a)

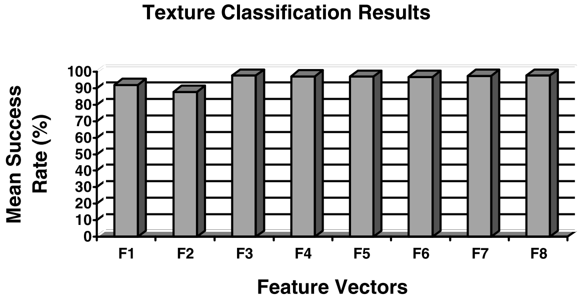

(b)

Fig. 4. Texture classification results—graphical analysis (Feat-DB1 (F1, F2 and F3); Feat-DB2 (F4); Feat-DB3 (F5, F6, F7 and F8)).

(iii) When feature database 3 is used, the highest mean success rate (i.e., 97.80%) is obtained with averaged feature sub-database of 256×256 image regions.

Further, it is important to note that a mean success rate of 97.68% is obtained with feature database 1, which is trained by only 20 original 512×512 texture images, while it is improved to 97.80% (i.e., an increase of 0.12% only) with feature database 3, which is trained by 1680 image regions of different sizes. Hence, it is finally concluded that the highest mean success rate is obtained with feature database 3, particularly for database of 256×256 image regions and comparable performance is achieved with less complex feature database 1.

Our current work has so far focused on algorithmic development and experimental justification. More thorough theoretical analysis is expected in the future. The effect of changing wavelets, on the texture classification system performance and the application of wavelet transform to texture segmentation are under our current investigation and the research work is under progress.

Acknowledgements

The authors are grateful to the Management, Principal and Head of the Department of Electronics and Communication Engineering of our college for their constant support and encouragement. The authors also extend their gratitude to the anonymous reviewers who have given very good suggestions for this better presentation of our manuscript.

Appendix A

$$\text{Contrast} = \sum_{i,j=1}^{N} (i-j)^2 C(i,j) \tag{A.1}$$

$$\text{Energy} = \sum_{i,j=1}^{N} C^2(i,j) \tag{A.2}$$

$$\text{Entropy} = -\sum_{i,j=1}^{N} C(i,j) \log_2 C(i,j) \tag{A.3}$$

$$\text{Local homogeneity} = \sum_{i,j=1}^{N} \frac{1}{1+(i-j)^2} C(i,j) \tag{A.4}$$

$$\text{Cluster shade} = \sum_{i,j=1}^{N} \left(i - M_x + j - M_y\right)^3 C(i,j) \tag{A.5}$$

$$\text{Cluster prominence} = \sum_{i,j=1}^{N} \left(i - M_x + j - M_y\right)^4 C(i,j) \tag{A.6}$$

$$\text{Maximum probability} = \text{Max}[C(i,j)] \tag{A.7}$$

where

$$M_x = \sum_{i,j=1}^{N} iC(i,j) \quad \text{and} \quad M_y = \sum_{i,j=1}^{N} jC(i,j).$$

References

Bovik, A., Clark, M., Geisler, W.S., 1990. Multichannel texture analysis using localized spatial filters. IEEE Trans. Pattern Anal. Machine Intell. 12, 55–73.

Chang, T., Jay Kuo, C.C., 1993. Texture analysis and classification with tree-structured wavelet transform. IEEE Trans. Image Process. 2 (4), 429–440.

Chellappa, R., Chatterjee, S., 1986. Classification of textures using Gaussian Markov random fields. IEEE Trans. Acoustics Speech Signal Process. ASSP-33 (4), 959–963.

Chen, P.C., Pavlidis, T., 1983. Segmentation by texture using correlation. IEEE Trans. Pattern Anal. Machine Intell. PAMI-5, 64–69.

Cohen, F.S., Fan, Z., Patel, M.A., 1991. Classification of rotation and scaled textured images using Gaussian Markov random field models. IEEE Trans. Pattern Anal. Machine Intell. 13 (2), 192–202.

Cross, G.R., Jain, A.K., 1983. Markov random field texture models. IEEE Trans. Pattern Anal. Machine Intell. PAMI-5 (1), 25–39.

Davis, L.S., Johns, S.A., Aggarwal, J.K., 1979. Texture analysis using generalized co-occurrence matrices. IEEE Trans. Pattern Anal. Machine Intell. PAMI-1, 251–259.

Derin, H., Elliot, H., 1987. Modeling and segmentation of noisy and textured images using Gibbs random fields. IEEE Trans. Pattern Anal. Machine Intell. PAMI-9, 39–59.

Faugeras, O.D., Pratt, W.K., 1980. Decorrelation methods of texture feature extraction. IEEE Trans. Pattern Anal. Machine Intell. PAMI-1, 323–332.

Haley, G.M., Manjunath, B.S., 1995. Rotation invariant texture classification using modified Gabor filters. Proc. IEEE, 262–265.

Haralick, R.M., Shanmugam, K., Dinstein, I., 1973. Texture features for image classification. IEEE Trans. System Man Cybernat. 8 (6), 610–621.

Kaplan, L.M., 1999. Extended fractal analysis for texture classification and segmentation. IEEE Trans. Image Process. 8 (11), 1572–1585.

Kashyap, R.L., Khotanzed, A., 1986. A model based method for rotation invariant texture classification. IEEE Trans. Pattern Anal. Machine Intell. PAMI-8 (4), 472–481.

Laws, K.L., 1980. Rapid texture identification. Proc. SPIE 238, 376–380.

Manjunath, B.S., Chellappa, R., 1991. Unsupervised texture segmentation using Markov random fields. IEEE Trans. Pattern Anal. Machine Intell. 13, 478–482.

Manjunath, B.S., Ma, W.Y., 1996. Texture features for browsing and retrieval of image data. IEEE Trans. Pattern Anal. Machine Intell. 18 (8), 837–842.

Raghu, P.P., Yegnanarayana, B., 1996. Segmentation of Gabor filtered textures using deterministic relaxation. IEEE Trans. Image Process. 5 (12), 1625–1636.

Sklansky, J., 1978. Image segmentation and feature extraction. IEEE Trans. System Man Cybernat. 8, 237–247.

Teuner, A., Pichler, O., Hosficka, B.J., 1995. Unsupervised texture segmentation of images using tuned matched Gabor filters. IEEE Trans. Image Process. 4 (6), 863–870.

Unser, M., 1986. Local linear transforms for texture measurements. Signal Process. 11, 61–79.

Unser, M., 1995. Texture classification and segmentation using wavelet frames. IEEE Trans. Image Process. 4 (11), 1549–1560.

Unser, M., Eden, M., 1989. Multiresolution feature extraction and selection for texture segmentation. IEEE Trans. Pattern Anal. Machine Intell. 2, 717–728.

Van de Wouwer, G., Schenders, P., Van Dyek, D., 1999. Statistical texture characterization from discrete wavelet representation. IEEE Trans. Image Process. 8 (4), 592–598.

VisTex, 1995, "Color image database", at http://www.white.media.mit.edu/vismod/imagery/VisionTexture, MIT media Lab.

Wang, L., Liu, J., 1999. Texture classification using multi resolution Markov random field models. Pattern Recog. Lett. 20 (2), 171–182.

Weszka, J.S., Dyer, C.R., Rosenfeld, A., 1976. A comparative study of texture measures for terrain classification. IEEE Trans. System Man Cybernat. SMC-6 (4), 269–286.

Wu, W.-R., Wei, S.-C., 1996. Rotation and gray scale transform invariant texture classification using spiral resampling, sub band decomposition and Hidden Markov model. IEEE Trans. Image Process. 5 (10), 1423–1433.